AD-A142 473 EFFECT OF TURBULENT BOUNDARY LAYER FLOW ON MEASUREMENT OF ACOUSTIC PRESSU..(U) PENNSYLVANIA STATE UNIV UNIVERSITY PARK APPLIED RESEARCH LAB.. G C LAUCHLE

UNCLASSIFIED 18 MAY 84 ARL/PSU/TM-84-87 N00024-79-C-6043 F/G 20/4 NL

1/1

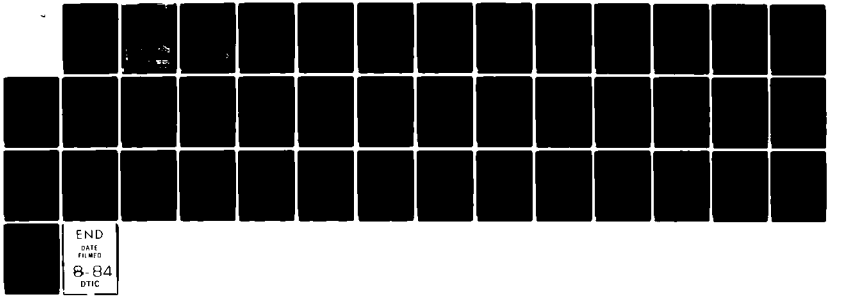

END
DATE FILMED
8-84
DTIC

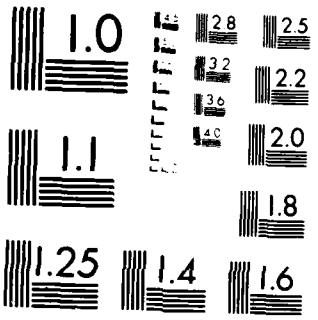

EFFECT OF TURBULENT BOUNDARY LAYER FLOW ON MEASUREMENT OF ACOUSTIC PRESSURE AND INTENSITY [REVISED]

G. C. Lauchle

Technical Memorandum
File No. TM 84-87
18 May 1984
Contract N00024-79-C-6043

Copy No. 39

The Pennsylvania State University
Intercollege Research Programs and Facilities
APPLIED RESEARCH LABORATORY
Post Office Box 30
State College, PA 16804

NAVY DEPARTMENT
NAVAL SEA SYSTEMS COMMAND

84 06 26 136

EFFECT OF TURBULENT BOUNDARY LAYER FLOW ON MEASUREMENT OF ACOUSTIC PRESSURE AND INTENSITY [REVISED]

G. C. Lauchle

Technical Memorandum
File No. TM 84-87
18 May 1984
Contract N00024-79-C-6043

Copy No. 39

The Pennsylvania State University
Intercollege Research Programs and Facilities
APPLIED RESEARCH LABORATORY
Post Office Box 30
State College, PA 16804

NAVY DEPARTMENT

NAVAL SEA SYSTEMS COMMAND

UNCLASSIFIED

SECURITY CLASSIFICATION OF THIS PAGE (When Data Entered)

REPORT DOCUMENTATION PAGE		READ INSTRUCTIONS BEFORE COMPLETING FORM
1 REPORT NUMBER TM 84-87	2. GOVT ACCESSION NO. AD-A142 473	3 RECIPIENT'S CATALOG NUMBER
4. TITLE (and Subtitle) EFFECT OF TURBULENT BOUNDARY LAYER FLOW ON MEASUREMENT OF ACOUSTIC PRESSURE AND INTENSITY [REVISED]		5 TYPE OF REPORT & PERIOD COVERED Technical Memorandum 6 PERFORMING ORG. REPORT NUMBER
7 AUTHOR(s) G. C. Lauchle		8 CONTRACT OR GRANT NUMBER(s) N00024-79-C-6043
9 PERFORMING ORGANIZATION NAME AND ADDRESS Applied Research Laboratory Post Office Box 30 State College, PA 16804		10 PROGRAM ELEMENT, PROJECT, TASK AREA & WORK UNIT NUMBERS
11. CONTROLLING OFFICE NAME AND ADDRESS Naval Sea Systems Command, Code NSEA 63R31 Department of the Navy Washington, DC 20362		12. REPORT DATE 18 May 1984 13. NUMBER OF PAGES 39
14. MONITORING AGENCY NAME & ADDRESS(if different from Controlling Office)		15. SECURITY CLASS. (of this report) Unclassified 15a. DECLASSIFICATION DOWNGRADING SCHEDULE

16. DISTRIBUTION STATEMENT (of this Report)

Approved for public release. Distribution unlimited.
Per NAVSEA - 13 June 1984.

17. DISTRIBUTION STATEMENT (of the abstract entered in Block 20, if different from Report)

18. SUPPLEMENTARY NOTES

19. KEY WORDS (Continue on reverse side if necessary and identify by block number)

turbulent boundary layer flow
acoustic pressure
intensity

20 ABSTRACT (Continue on reverse side if necessary and identify by block number)

Acoustic measurements performed with pressure sensors (microphones and hydrophones) can be subject to misinterpretation if the sensors are in contact with a turbulent boundary layer flow. This misinterpretation is a result of non-propagating pressure fields (flow noise) generated by the turbulent motions of the fluid. In this paper, a simple analysis is given whereby the flow noise response of a pressure sensor placed in a turbulent boundary layer flow can be estimated. If the purpose of the →

DD FORM 1 JAN 73 1473 EDITION OF 1 NOV 65 IS OBSOLETE

UNCLASSIFIED

SECURITY CLASSIFICATION OF THIS PAGE (When Data Entered)

sensor is to measure the sound emitted from an independent source outside of the turbulent boundary layer, then a bias for the measurement can be calculated. A bias formula for intensity measurements made with two-sensors under a turbulent boundary layer is also derived under the assumption of a very low Mach number flow.

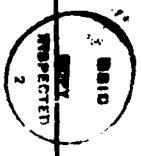

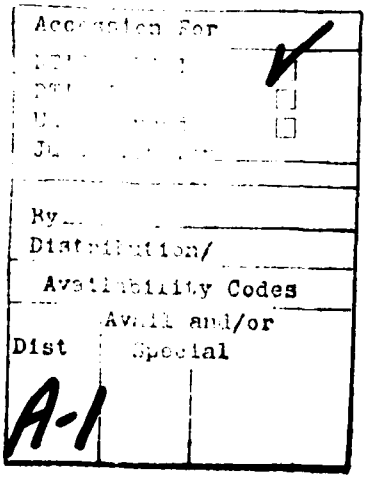

From: G. C. Lauchle

Subject: Effect of Turbulent Boundary Layer Flow on Measurement of Acoustic Pressure and Intensity (Revised)

Preface: Because of an error, ARL/PSU TM 83-163 has been revised. This error is significant enough to alter the conclusions, so it is necessary to re-issue a revised version of the report which is contained herein. Please discard ARL/PSU TM 83-163, and use this version in its place.

Abstract: Acoustic measurements performed with pressure sensors (microphones and hydrophones) can be subject to misinterpretation if the sensors are in contact with a turbulent boundary layer flow. This misinterpretation is a result of non-propagating pressure fields (flow noise) generated by the turbulent motions of the fluid. In this paper, a simple analysis is given whereby the flow noise response of a pressure sensor placed in a turbulent boundary layer flow can be estimated. If the purpose of the sensor is to measure the sound emitted from an independent source outside of the turbulent boundary layer, then a bias for the measurement can be calculated. A bias formula for intensity measurements made with two-sensors under a turbulent boundary layer is also derived under the assumption of a very low Mach number flow.

Acknowledgement: This work has been performed at the Applied Research Laboratory of The Pennsylvania State University under contract with the Naval Sea Systems Command, Code NSEA 63R31. Mr. Mark Daniels is thanked for his help in the computer programming.

INTRODUCTION

There has been considerable interest recently in the measurement of acoustic pressure and acoustic intensity in ducting systems and other systems that sustain a mean flow [1-5]*. The work of Munro and Ingard [3] is fundamental and provides a mathematical description of acoustic intensity for a medium in motion. They point out that two potential problems exist when one attempts to measure intensity in a system with flowing fluid. The first deals with the definition of intensity, where the majority of their paper addresses this issue. The second problem deals with what, exactly, does a pressure sensor (microphone or hydrophone) which is placed in a flow field measure? This problem is associated with "wind noise" or "flow noise" and is not discussed further in Ref. [3].

For the experimentalist, flow noise can be an important problem that deserves some attention. It must be pointed out that it is a difficult problem to solve, in general, because each situation is likely to have unique features associated with the flow field, and with the acoustical measurement apparatus. In an attempt to generalize the latter, we can usually envision the measurement sensors to be situated either in the free stream, or somehow flush mounted in the walls of the system. For example, measurements of tire noise may be conducted on a moving vehicle with a microphone placed in the free stream near the tire and roadway. This situation is discussed by Oswald and Donavan [4], where the errors due to the probes being in a free stream are assessed. They conclude that very good accuracy is achieved with intensity probes for those situations in which the flow Mach number is less

*Numbers in brackets denote references listed at the end of the paper.

than 0.1 and the turbulence intensity is less than about 5 percent. These results are based on anechoic wind tunnel measurements using microphones equipped with streamlined nose cones.

The effect of turbulence-induced noise on flush-mounted sensors has been of concern to those involved in underwater sonar system design and evaluation, and to researchers that utilize wind or water tunnel test facilities in aero and hydroacoustic investigations, e.g., [6-8]. The predominant source of this noise is the turbulent boundary layer that exists between the walls of the system and the free stream. Boundary layer turbulence produces pressure flucutations that span wide frequency and wavenumber ranges. The response of a flush-mounted sensor placed beneath a turbulent boundary layer depends therefore on the details of the boundary layer wavenumber/frequency pressure spectrum and on its own spatial averaging characteristics. One of the first mathematical descriptions of this type of interaction is given by Uberoi and Kovasznay [9].

Many noise control engineering problems involve the measurement of an acoustical phenomenon associated with fluid moving devices or systems. Such problems include the diagnosis and reduction of noise sources of aircraft, ships, cooling/heating systems, and hydraulic systems, to name a few. Other problems are associated with the evaluation of materials or products that are to be subjected to flow. This latter area has led to the recent interest in duct-type test facilities [1,5]. The identification of boundary layer-induced transducer response would be of interest in most of those applications that use flush-mounted sensors. In this paper, a simple analysis of this type of response is presented. The analysis makes use of research findings in several disciplines: hydrodynamics, hydroacoustics, and acoustics. Well-

known concepts of each discipline are combined to provide a useful method for estimating a bias that can exist in such measurements. Numerical examples are presented for typical transducer sizes and air flow velocities encountered in practice.

PRELIMINARIES

The problem to be investigated is the determination of that portion of a pressure or intensity spectrum due to turbulent boundary layer pressure fluctuations when the measurement is performed under a turbulent boundary layer with flush pressure sensors of given shape and size. For convenience, this problem is approached using a planar surface as a model. The results obtained with this model may be extended to duct flow problems providing that the appropriate changes in turbulent boundary layer development are accounted for.

Flow Considerations

Consider the planar flow model of Figure 1. The mean flow velocity is denoted by u_0 and it is assumed that $u_0/c = M < 0.1$, where c is the sonic velocity. The fluid (air, water, oil, etc.) is characterized by its viscosity, μ, and density, ρ. The kinematic viscosity is $\nu = \mu/\rho$. A parameter which helps classify the dynamic similarity of geometrically similar flows is the Reynolds number, $Re_\ell = u_0\ell/\nu$. Here, ℓ is a characteristic length of the plate, tube, or body. In the case of viscous flow over a surface (Figure 1), a shear layer develops very close to the surface. In traditional descriptions of this boundary layer, the length used in the Reynolds number may be either the streamwise coordinate, x_1, or the thickness of the layer, δ. The boundary layer is defined as that region

above the surface where the velocity, u depends on x_2. Its thickness, δ, is defined at that value of x_2 where $u = 0.99\ u_0$. In some instances, the mean velocity may be directed at some angle to the plane. In these cases, a mean pressure gradient will exist along the surface and alternative definitions for the boundary layer flow are necessary. For the analysis of this paper, it is assumed that the flow is parallel to the surface.

Initially, near the leading edge, the boundary layer is laminar. The streamlines are straight and parallel in the boundary layer and no fluctuations in velocity or pressure are produced. The laminar layer persists for only short distances before instabilities arise and the layer "transitions" into a turbulent layer. The transition location for a smooth flat plate can be estimated from the transition Reynolds number, typically in the range [10]: $10^5 \leq Re_{x_t} \leq 10^6$. In the case of a smooth pipe flow, $Re_{x_t} \approx 2300$, where the velocity, u_0, is that at the center of the pipe. The transition location is sensitive to surface finish. In general, these transition Reynolds numbers would be much lower for rough surfaces. The turbulence in the layer is assumed homogeneous and of zero mean.

Acoustic Measurement Considerations

It is assumed that pressure sensitive transducers are mounted flush in a surface as illustrated in Figure 1. It is further assumed that the purpose of these sensors is to measure an acoustic field (either the pressure or the intensity vector), and that this field is statistically independent of the pressure field generated by the turbulent layer. The rms acoustic pressure originating from the source of interest is denoted by p_a and is sensed by a single transducer. The turbulence produces rms pressure p_T which together

with p_a results in a total measured pressure:

$$p = p_a + p_T \quad . \tag{1}$$

The acoustic intensity, I_a, is determined in the usual way using a pair of sensors located a distance Δx apart [11,12]:

$$I_a \simeq - \mathrm{Im}(G_{12})/\rho\omega\Delta x \quad . \tag{2}$$

Equation (2) contains the quad-spectrum $(\mathrm{Im}G_{12})$ as measured by the pair of transducers, and ω is the radian frequency. It is assumed that all corrections for sensitivity and phase mismatch have been accounted for.

BIAS DUE TO TURBULENT BOUNDARY LAYER FLOW

If our objective is to measure either p_a or I_a in the presence of a turbulent boundary layer (TBL), Equation (1) shows that this measurement may be biased. If $\hat{\theta}$ is a measured quantity, and θ is the desired or true quantity, then the bias is defined [13] as:

$$b(\hat{\theta}) = E\{\hat{\theta}\} - \theta \quad , \tag{3}$$

where $E\{\ \}$ denotes expectation operation. The normalized bias is $b(\hat{\theta})/\theta$.

Pressure Spectrum Measurement

The one-sided power spectrum measured by a single flush-mounted sensor is defined [13] as

$$G_{pp}(\omega) = \lim_{T\to\infty} \frac{2}{T} E\{P^* P\} \quad , \tag{4}$$

where P is the finite Fourier transform of p and the asterick denotes complex conjugate. Using Equation (1) in Equation (4) results in:

$$G_{pp} = G_{aa} + G_{TT} + G_{aT} + G_{Ta} \quad ,$$

where G_{aT} and G_{Ta} are cross spectra between the TBL-induced pressure and the acoustic pressure. Because of statistical independence, these two cross spectra are zero, and

$$G_{pp} = G_{aa} + G_{TT} \quad . \tag{5}$$

An estimate for the acoustic pressure autospectrum is $\hat{G}_{aa}(\omega)$, so the bias in this estimate follows directly:

$$b\{\hat{G}_{aa}\} = E\{\hat{G}_{aa}\} - G_{aa}$$

$$= G_{aa} + G_{TT} - G_{aa}$$

$$b\{\hat{G}_{aa}\} = G_{TT} \quad . \tag{6}$$

The normalized bias is:

$$\epsilon_b\{\hat{G}_{aa}\} = G_{TT}/G_{aa} \quad . \tag{7}$$

Equation (7) is an expected result for two independent sources; it states that the normalized bias error for the acoustic autospectrum is simply a noise-to-signal ratio, where the spectrum of the turbulent boundary layer pressure field represents the noise term. In practice, the numerator might possibly be determined by turning off the acoustical source while retaining the flow. When this is not possible, G_{TT} can be estimated by procedures

given in Appendix A. Likewise, the denominator of Equation (7) could be determined by measuring the acoustic autospectrum in the absence of flow. When this is not possible, the normalized bias for $\hat{G}_{aa}$ can still be computed with a knowledge of G_{pp} and Equation (5), i.e.,

$$\varepsilon_b(\hat{G}_{aa}) = (G_{TT}/G_{pp})/(1 - G_{TT}/G_{pp}) \quad . \tag{8}$$

Intensity Spectrum Measurement

Letting $\hat{I}_a(\omega)$ be the intensity spectrum calculated from measurements made with the pair of sensors (labeled 1 and 2) sketched in Figure 1, it follows that:

$$b(\hat{I}_a) = - \operatorname{Im}(\hat{G}_{12})/\rho\omega\Delta x + \operatorname{Im}(G_{12})/\rho\omega\Delta x \quad . \tag{9}$$

Here, $\hat{G}_{12}$ is the measured cross spectrum between the two sensors with flow and G_{12} would be the cross spectrum measured in the absence of flow. Noting that

$$\hat{p}_1 = p_{a_1} + p_{T_1} \tag{10a}$$

and

$$\hat{p}_2 = p_{a_2} + p_{T_2} \quad , \tag{10b}$$

where subscripts 1 and 2 refer to sensors 1 and 2 respectively, we find that

$$\hat{G}_{12} = G_{12} + G_{T_1T_2} + G_{a_1T_2} + G_{T_1a_2} \quad . \tag{11}$$

Again, because of the statistical independence between p_a and p_T, Equation (11) reduces to:

$$\hat{G}_{12} = G_{12} + G_{T_1T_2} \quad . \tag{12}$$

If the two sensors are placed farther apart than the streamwise correlation length, A, of the turbulent pressure fluctuations, then the turbulence-induced cross spectrum $G_{T_1T_2}$ is nearly zero. It would be concluded then [Equation (9)] that the estimate for the acoustic intensity is unbiased when the measurement is performed under a TBL. It is presumed that the measurements of Oswald and Donavan [4] were performed using probe separations greater than the correlation lengths of the turbulent pressure fluctuations that occur in the free stream of the wind tunnel used. That is why they found very little error in the intensity measurements even when the noise-to-signal ratio for the noisiest microphone was greater than unity. Nonetheless, it is important to examine Equation (9) in some detail in an attempt to identify those ranges of turbulence length scales where $G_{T_1T_2}$ cannot be neglected.

The cross spectrum of the pressure fluctuations that occur at the wall under a TBL was modeled by Corcos [6] and others. For this discussion, the Corcos model is sufficiently accurate and accounts for the spatial averaging effects introduced by the finite size of the measurement sensors. This model states that the measured cross spectrum is of the form:

$$G_{T_1T_2}(\omega,\xi,\eta) \cong G_{TT}(\omega)A(k_c\xi)B(k_c\eta)e^{-ik_c\xi} \quad . \tag{13}$$

Here, ξ represents the separation of the two sensors in the x_1-direction and η is the separation in the spanwise (x_3) direction (assumed to be zero for this study). The wavenumber k_c is ω/u_c and is called the convection wavenumber since u_c represents the speed at which the pressure producing turbulence is "convected" over the surface. This process is, in general, dispersive with u_c being a weak function of ω. However, the dependence is slight and many workers in the field assume (as we will here) that $u_c \approx 0.7\ u_0$. The functions A and B are normalized and can be approximated by:

$$A(k_c\xi) \approx \exp(-\ 0.115|k_c\xi|) \tag{14}$$

$$B(k_c\eta) \approx \exp(-\ 0.7|k_c\eta|) \quad . \tag{15}$$

With the intensity probe oriented in the direction of flow, $\xi = \Delta x$ and $\eta = 0$; thus, the imaginary part of $G_{T_1T_2}$ is of the form:

$$\mathrm{Im}(G_{T_1T_2}) \approx -\ G_{TT}(\omega)A(k_c\Delta x)\sin\ k_c\Delta x \quad . \tag{16}$$

We can now use Equation (12) in Equation (9) to obtain:

$$b(\hat{I}_a) \approx -\ \mathrm{Im}(G_{T_1T_2})/\rho\omega\Delta x$$

$$\approx [G_{TT}(\omega)A(k_c\Delta x)\sin\ k_c\Delta x]/\rho\omega\Delta x$$

or,

$$b\left(\hat{I}_a\right) \approx \frac{G_{TT}(\omega)}{\rho u_c} \Lambda(k_c \Delta x) \frac{\sin k_c \Delta x}{k_c \Delta x} \quad . \tag{17}$$

A non-dimensionalized plot of this bias is given in Figure 2 where $k_c \Delta x$ is the independent variable. A second axis, $\Delta x/\Lambda$ is also shown, where the correlation length is calculated from:

$$\Lambda = \int_0^\infty \Lambda(k_c \xi) d\xi$$

$$\Lambda \approx 11\pi/4k_c \quad . \tag{18}$$

(The accepted form of the correlation length is based on the magnitude of the cross spectrum.) This plot shows clearly the rapid decorrelation of turbulent energy as $\Delta x/\Lambda$ increases. From it we can conclude that an intensity spectrum estimate would be essentially unbiased for sensor separations greater than about one TBL correlation length (Λ). Because of Equation (18), we must recognize that Λ is inversely related to frequency such that a bias can exist in intensity measurements for low frequencies (f_L), i.e.,

$$f_L < \frac{11}{8} \frac{u_c}{\Delta x} \qquad (u_c \approx 0.7\ u_0) \quad . \tag{19}$$

Below f_L, the magnitude of this bias may still be small because of the multiplicative factor $G_{TT}/\rho u_c$ of Equation (17). This magnitude can be qualified conveniently by examining the normalized bias.

For the assumed propagating acoustic field,

$$I_m(G_{12}) = |G_{12}| \sin k\Delta x \quad , \tag{20}$$

where k is the sonic wavenumber. But, the finite difference criterion for the two-sensor intensity method requires $k\Delta x \ll 1$. Therefore, we can let $\sin k\Delta x \approx k\Delta x$. Then, the normalized bias is:

$$\varepsilon_b(\hat{I}_a) \approx \frac{1}{M_c} \frac{G_{TT}}{|G_{12}|} A(k_c\Delta x) \frac{\sin k_c\Delta x}{k_c\Delta x} \quad , \tag{21}$$

where M_c is introduced as the convective Mach number (u_c/c). From Equations (17) and (21), the ordinate of Figure 2 is also interpreted as:

$$\frac{b(\hat{I}_a)\rho u_c}{G_{TT}} = \varepsilon_b(\hat{I}_a) M_c \frac{|G_{12}|}{G_{TT}} \quad . \tag{22}$$

As an example, if $\Delta x/\Lambda = 1.0$, Equation (22) would have a numerical value of order 0.01. If the air velocity is on the order of 30 m/s, where $M = 0.1$ (above this, the intensity definition used becomes invalid [3]) and $M_c \approx 0.07$, we see that

$$\varepsilon_b(\hat{I}_a) \approx \frac{1}{7} \frac{G_{TT}}{|G_{12}|} \quad .$$

Clearly, $\varepsilon_b(\hat{I}_a)$ is only 14 percent for the extreme condition of $G_{TT} = |G_{12}|$. If Δx is much larger than Λ, these results suggest that accurate intensity measurements can be performed under a TBL even when the sensed TBL auto-spectral density is higher than that due to the acoustic source. That is, the normalized bias for $\hat{G}_{aa}$ [Equation (7)] could be as much as two orders of

magnitude higher than the normalized bias for $\hat{I}_a$. As pointed out by Corcos [6], and detailed in Appendix A, these biases can be reduced significantly by using large diameter microphones in the measurements.

CONCLUSIONS

In this paper, an analysis is given for a potential data interpretation error that may occur in acoustical measurements that employ pressure sensors mounted in walls of systems that sustain low-Mach number flow. A review of recent literature reveals that measurements of this type are conducted in the noise control engineering field, so it appears that an analysis of this type may be of interest. Under the assumptions that the flow Mach number is low (so that the zero-flow definition of intensity may be used), and that the pressure fluctuations generated by the turbulent boundary layer flow are statistically independent of the acoustical pressure under investigation, the normalized bias expected in the measurement of the acoustical autospectrum is shown to be simply a noise-to-signal ratio. The bias in the intensity spectrum is shown to be significantly smaller than this noise-to-signal ratio provided that the sensor separation is greater than the streamwise correlation length of the pressure fluctuations created in the turbulent boundary layer.

Methods for predicting the TBL wall pressure spectrum as measured by transducers of finite size are given in an Appendix along with example calculations. For the typical air flow velocities and sensor sizes encountered in practice, these example calculations show that the measurement of acoustical pressures that are lower than approximately 60 dB re 20μPa/ Hz will be influenced by the presence of a TBL.

The limitations of the analysis, in addition to those associated with the assumptions, include the following:

(1) Vibration of the surface may lead to sensor response not accounted for in the analysis. This would be most critical for liquid flows where fluid loading is non-negligible.

(2) Angle of attack effects may require modifications in the flow equations and pressure spectrum analyses of Appendix A.

APPENDIX A

Estimation of $G_{TT}(\omega)$

Equations (7), (8), (17) and (21) all contain $G_{TT}(\omega)$ which is the auto-spectrum of the TBL pressure fluctuations as measured by a flush-mounted pressure sensor of given physical size. If the source of interest can be turned off while still retaining the TBL flow, then $G_{TT}(\omega)$ can be measured directly; otherwise, it must be estimated from theoretical analysis. This appendix gives such an analysis.

The wall pressure spectrum is calculated from methods first presented by Uberoi and Kovasznay [9]. In particular:

$$G_{TT}(\omega) = \int_{-\infty}^{\infty}\int_{-\infty}^{\infty} \Phi(k_1,k_3,\omega)|H(k_1,k_3)|^2 dk_1 dk_3 \quad , \tag{A-1}$$

where $|H(k_1,k_3)|^2$ is the in-plane wavenumber response function of the sensor, and $\Phi(k_1,k_3,\omega)$ is the wavenumber/frequency spectrum of the TBL wall pressure fluctuations at the given Reynolds number.

The sensor spatial response function depends on the shape of the sensor. Most microphones and hydrophones used in pressure and intensity measurements are circular. For circular elements of active diameter, D = 2R,

$$|H(kR)|^2 = [2J_1(kR)/kR)]^2 \quad , \tag{A-2}$$

where $k^2 = k_1^2 + k_3^2$, and J_1 is the Bessel function of order one. Figure 3 shows the variation of $|H(k_1R)|^2$ with k_1R. Because of polar symmetry, this variation is identical to that in the k_3R domain. The measured response

function shown in Figure 2 is by Farabee and Geib [14]. If rectangular elements are used in a given application [6],

$$|H(k_i L_i)|^2 = \sin^2(k_i L_i/2)/(k_i L_i/2)^2 \quad , \qquad \text{(A-3)}$$

$$i = 1,3 \quad ,$$

and L_i is the length of the side in direction x_i.

Over the past twenty years or more, many papers have been published on the wall pressure spectrum of turbulent boundary layers. Even today, disagreement exists among researchers as to the true form of this spectrum. Measurement of $\Phi(k_1,k_3,\omega)$ is extremely difficult because of its multi-dimensionality and its wide dynamic range. Likewise, theoretical modeling usually requires some experimental data in order to fix proportionality constants that arise.

Aside from these difficulties, the hydroacoustics community generally agrees that $\Phi(k_1,k_3,\omega)$ is a symmetric, gradually decreasing function in k_3, and varies in ω like narrow-band random noise. The variation of $\Phi(k_1,k_3,\omega)$ with k_1 (streamwise direction) is more complicated. Figure 4 is a schematic description of $\Phi(k_1,0,\omega)$. A sharp, well-defined peak occurs at the convection wavenumber. The peak is simply explained in terms of pressure pulses created by the eddies of turbulent flow that travel at speed u_c. Because the convective wavenumber is much greater than the sonic wavenumber (ω/c) by a factor of $O(M_c^{-1})$, energy at the convective peak is non-propagating. The only energy that propagates is that for which $k_1 < \omega/c$. The energy in the sonic wavenumber portion of the spectrum is very small in comparison to that in the high, convective wavenumber region.

A so-called low wavenumber region exists between the sonic and convection wavenumbers. The energy in this region is considered important because this band of wavenumbers $(\omega/c < k_1 < \omega/u_c)$ usually couples well with flexural wavenumbers of real structures. (The coupling is most efficient for underwater structures.) Figure 4(a) indicates a parabolic curve that relates the resonant frequency of a typical flat plate with wavenumber. The constant α is related to the bending stiffness of the plate.

Measurements of $\Phi(k_c,0,\omega)$ have been quite successful in recent years. Inspection of Equations (A-1) through (A-3) reveals that a measured spectrum would be dominated by the energy at $k_1 = k_c$ if very small pressure transducers were used to make the measurement. The spectra measured by Blake [15] with pinhole microphones on a plane surface in an air flow are quite representative of $\Phi(k_c,0,\omega)$.

Measurements in ranges where $k_1 < k_c$ are less common and very difficult to perform. Wavenumber filters are necessary in order to block out the contributions from the sonic and convective regions. Limited low wavenumber pressure spectra are given by Blake and Chase [8] and by Martin and Leehey [16].

In an attempt to formulate a model of $\Phi(k_1,k_3,\omega)$, Maestrello [17] measured space-time correlation functions of TBL pressure fluctuations with pairs of small microphones in a planar surface. These functions were then Fourier analyzed in both space and time to obtain the wavenumber/frequency spectrum. The Maestrello model is characterized by a low wavenumber region that remains flat with decreasing k_1. In a more recent analysis,

Chase [18] argues that the spectral level should eventually decrease to zero as $k_1 \to 0$. His model shows a k_1^{-2} dependence for $k_1 < k_c$ and is given by:

$$\Phi(k_1,k_3,\omega) = \rho^2 v_*^3 [C_M k_1^2 K_M^{-5} + C_T (k_1^2 + k_3^2) K_T^{-5}] \quad , \tag{A-4}$$

$$K_i = [(\omega - u_c k_1)^2 / h_i^2 v_*^2] + (k_1^2 + k_3^2) + (b_i \delta)^{-2} \quad , \tag{A-5}$$

$i = M,T$. The velocity, v_*, is the friction velocity and is related to the wall shear stress by $v_* = (\tau_w/\rho)^{1/2}$. For a smooth flat plate,

$$\tau_w \approx 0.029 \ \rho u_0^2 Re_{x_1}^{-1/5} \tag{A-6}$$

where the Reynolds number is based on the distance back from the beginning of the TBL. The TBL thickness at x_1 is approximated by:

$$\delta \approx 0.37 \ x_1 \ Re_{x_1}^{-1/5} \quad . \tag{A-7}$$

The constants of Equations (A-4) and (A-5) need to be selected through comparison of predictions with appropriate data. Chase considers the Martin-Leehey data [16] to be good at low wavenumbers. Also, using the Blake data for $k_1 = k_c$, the following constants are established:

$$h_M = h_T = 20.0 \quad , \quad C_M = 0.05 \quad , \quad C_T = 0.004 \quad ,$$

$$b_M = 0.75 \quad , \quad \text{and} \quad b_T = 0.38 \quad .$$

A comparison of the Chase and Maestrello models is given in Figure 5. Clearly, large differences are apparent, but it must be emphasized that both models depend to fair degree on the accuracy of the experimental data used in their development. Because the Chase model makes use of the data base obtained at very low Mach numbers, it is the recommended model for the analysis of this paper.

Equation (A-1) is solved by numerical integration for the flow conditions considered by Blake [15] in his measurements of $\Phi(k_c,0,\omega)$. The integrations are terminated at $(-10\ k_c,\ 10\ k_c)$ for both variables. The microphone diameter used by Blake is 0.79 mm (pinhole cap over standard B&K 4138 microphone), and his airflow velocities range from 22.2 to 50 m/s. A comparison of Blake's data for 22.5 m/s $(Re_{x_1} = 4.33 \times 10^5)$ with the prediction using the Chase model for $\Phi(k_1,k_3,\omega)$ is given in Figure 6. The agreement is reasonably good, except for low frequencies, where differences of order 6 dB occur. Calculations at other velocities compare equally well with the experimental spectra.

To further illustrate the types of sensor response expected when the sensor is placed under a TBL, Figure 7 is shown. Three typical Reynolds numbers are selected which would correspond to air velocities (standard temperature and pressure) of 6.10, 18.29, and 24.38 m/s at a streamwise sensor location of $x_1 = 0.30$ m. Spectra, for four microphones of diameter ranging from 3.18 to 25.4 mm are shown. These predicted spectra are essentially flat up to a cutoff frequency which is dependent upon the microphone diameter and the Reynolds number. This cutoff frequency decreases as the sensor diameter increases because the spatial averaging characteristics or larger sensors tends to cancel out much of the

convective wavenumber portion of the wavenumber/frequency spectrum. These examples illustrate that the overall level of G_{TT} is lowest for the larger measurement sensors; a result predicted previously by Corcos [6]. Above the cutoff frequency, the spectral level decreases approximately as ω^{-3}.

REFERENCES

1. Chung, J. Y. and D. A. Blaser, "Transfer Function Method of Measuring Acoustic Intensity in a Duct System with Flow," J. Acoust. Soc. Am., 68, 6, pp. 1570-1577 (1980).

2. Alfredson, R. J., "The Design and Optimization of Exhaust Silencers," Ph.D. Thesis, U. Southampton, England, July 1970.

3. Munro, D. H. and K. U. Ingard, "On Acoustic Intensity Measurements in the Presence of Mean Flow," J. Acoust. Soc. Am., 65, 6, pp. 1402-1406 (1979).

4. Oswald, L. J. and P. R. Donavan, "Acoustic Intensity Measurements in Low Mach Number Flows of Moderate Turbulence Levels," Gen. Motors Research Lab. Report GMR-3269, April 24, 1980.

5. Seybert, A. F. and D. F. Ross, "Experimental Determination of Acoustic Properties using a Two-Microphone Random Excitation Technique," J. Acoust. Soc. Am., 61, 5, pp. 1362-1370 (1977).

6. Corcos, G. M., "Resolution of Pressure in Turbulence," J. Acoust. Soc. Am., 35, 2, pp. 192-199 (1963).

7. Skudrzyk, E. J. and G. P. Haddle, "Noise Production in a Turbulent Boundary Layer by Smooth and Rough Surfaces," J. Acoust. Soc. Am., 32, 1, pp. 19-34 (1960).

8. Blake, W. K. and D. M. Chase, "Wavenumber-Frequency Spectra of Turbulent-Boundary-Layer Pressure Measured by Microphone Arrays," J. Acoust. Soc. Am., 49, 3, pp. 862-877 (1971).

9. Uberoi, M. S. and L. S. G. Kovasznay, "On Mapping and Measurement of Random Fields," Quart. Appl. Math., 10, 4, pp. 375-393 (1953).

10. Schlichting, H., Boundary-Layer Theory, 6th ed. (McGraw-Hill, 1968), pp. 432, 458, 599.

11. Fahy, F. J., "Measurement of Acoustic Intensity using the Cross-Spectral Density of Two Microphone Signals," J. Acoust. Soc. Am., 62, 4, pp. 1057-1059 (1977).

12. Chung, J. Y., "Cross-Spectral Method of Measuring Acoustic Intensity without Error Caused by Instrument Phase Mismatch," J. Acoust. Soc. Am., 64, 6, pp. 1613-1616 (1978).

13. Bendat, J. S. and A. G. Piersol, Engineering Applications of Correlation and Spectral Analysis (John Wiley & Sons, 1980), p. 38.

14. Farabee, T. M. and F. E. Geib, Jr., "Measurement of Boundary Layer Pressure Fields with an Array of Pressure Transducers in a Subsonic Flow," Proc. Int. Congress on Instr. in Aerosp. Sim. Facilities, Ottawa, Canada, September 1975, pp. 311-319.

15. Blake, W. K., "Turbulent Boundary-Layer Wall-Pressure Fluctuations on Smooth and Rough Walls," J. Fluid Mech., 44, 4, pp. 637-660 (1970).

16. Martin, N. C. and P. Leehey, "Low Wavenumber Wall Pressure Measurements using a Rectangular Membrane as a Spatial Filter," J. Sound and Vibra., 52, 1, pp. 95-120 (1977).

17. Maestrello, L., "Use of a Turbulence Model to Calculate the Vibration and Radiation Responses of a Panel, with Practical Suggestions for Reducing Sound Level," J. Sound and Vibra., 5, 3, pp. 407-448 (1967).

18. Chase, D. M., "Modeling the Wavevector-Frequency Spectrum of Turbulent Boundary Layer Pressure," J. Sound and Vibra., 70, 1, pp. 29-67 (1980).

LIST OF FIGURES

Figure 1. Schematic description of boundary layer flow over a flat surface that contains acoustical pressure measurement sensors. The wall is assumed to be rigid and u_0/c is assumed small, where c = sound speed.

Figure 2. Non-Dimensionalized bias for intensity estimate of Equation (17) as a function of $k_c\Delta x$ or $\Delta x/\Lambda$.

Figure 3. Wavenumber response function for circular sensor. The experimental curve is from Ref. [14].

Figure 4. Schematic description of the wavenumber/frequency spectrum, where (a) shows the $\omega - k_1$ plane and (b) shows the $\Phi - k_1$ plane.

Figure 5. Theoretical wavenumber/frequency spectra based on the models of Maestrello [17] and Chase [18].

Figure 6. A comparison of the wall pressure spectrum measured by Blake [15] with a theoretical prediction based on Equation (A-1) and the Chase [18] model for $\Phi(k_1,k_3,\omega)$.

Figure 7. Example calculations of $G_{TT}(\omega)$ for various values of the flow Reynolds number and for sensor diameters: (a) 25.40 mm, (b) 12.70 mm, (c) 6.35 mm, and (d) 3.18 mm.

ACOUSTIC INTENSITY, I_a

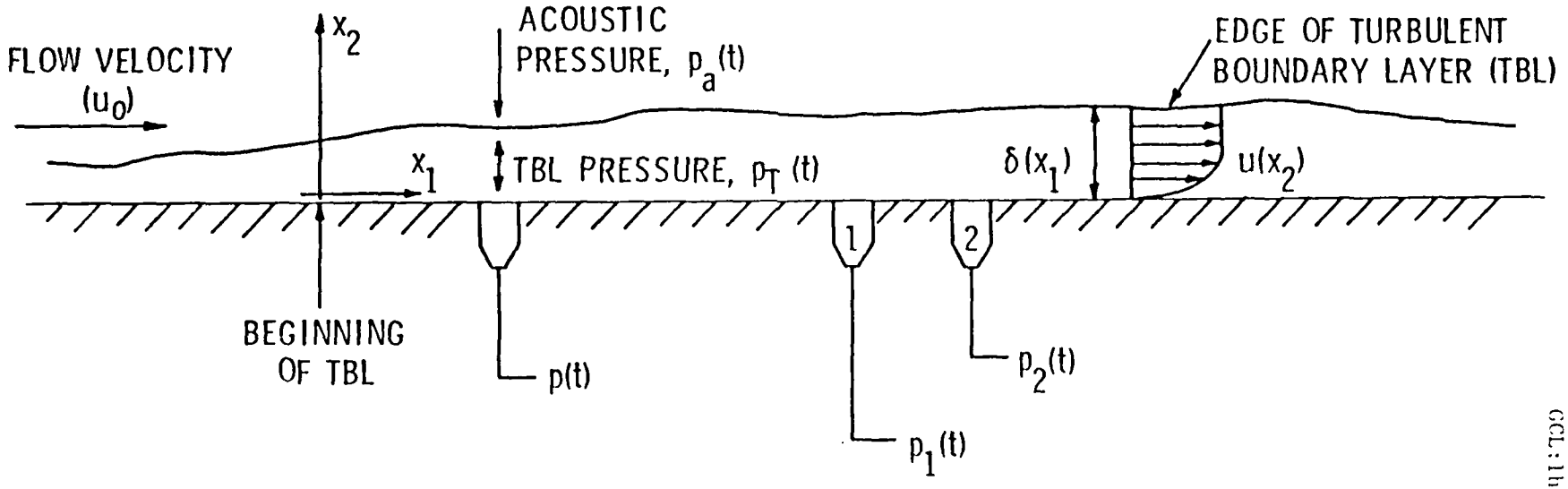

Figure 1. Schematic description of boundary layer flow over a flat surface that contains acoustical pressure measurement sensors. The wall is assumed to be rigid and u_0/c is assumed small, where c = sound speed.

18 May 1984
GCL:lhz

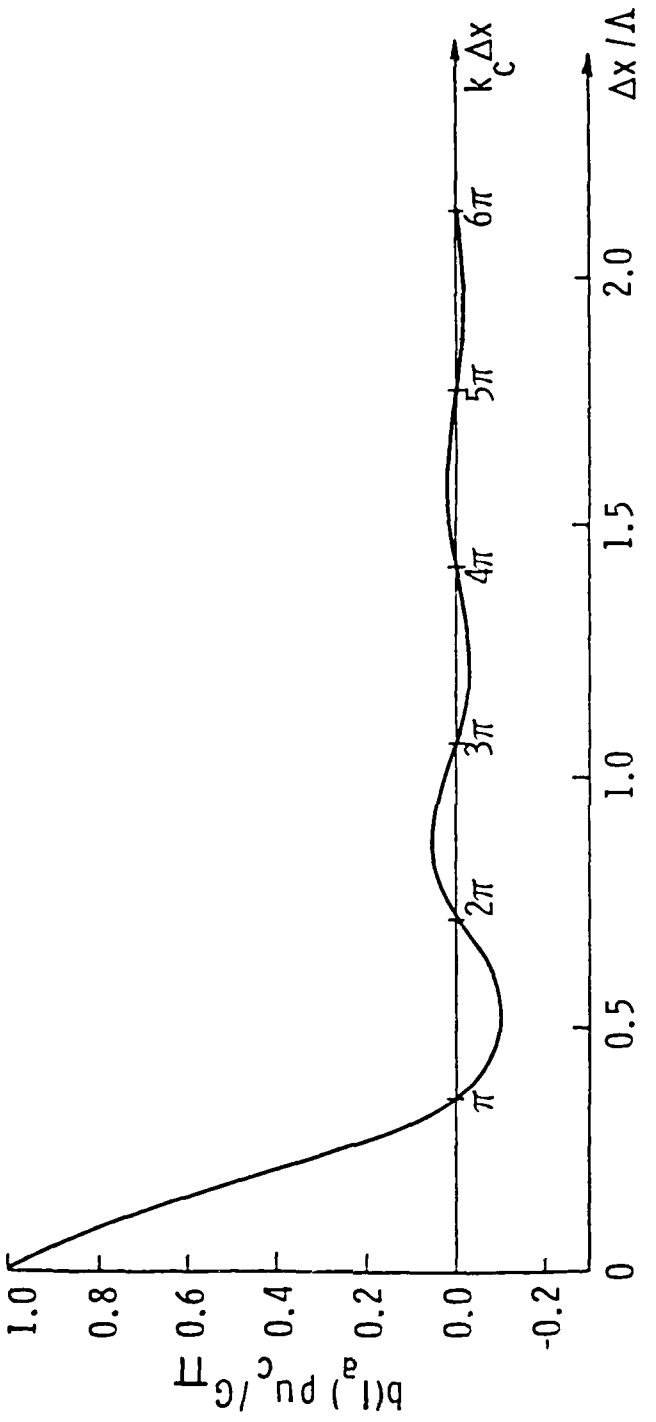

Figure 2. Non-Dimensionalized bias for intensity estimate of Equation (17) as a function of $k_c\Delta x$ or $\Delta x/\Lambda$.

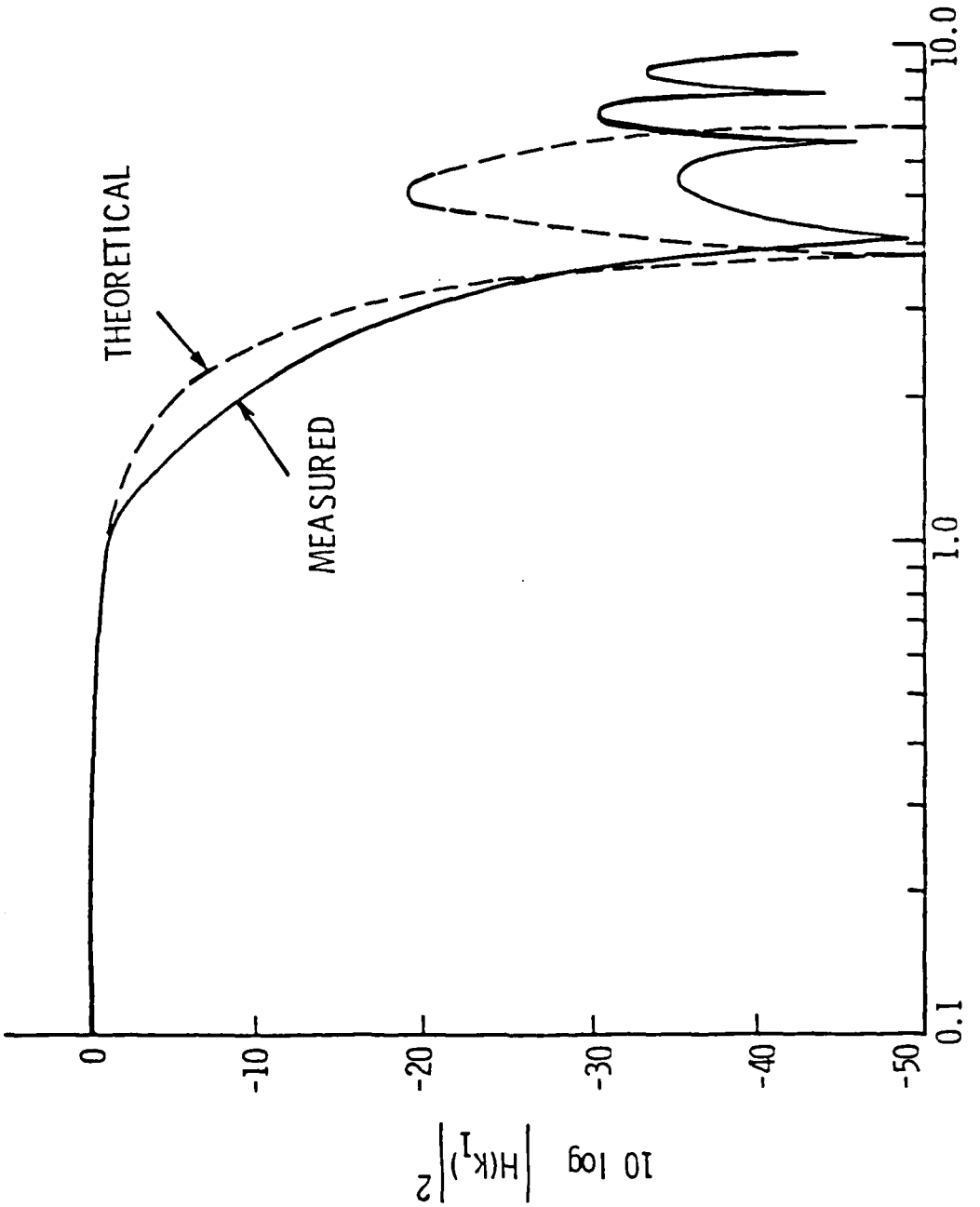

Figure 3. Wavenumber response function for circular sensor. The experimental curve is from Ref. [14].

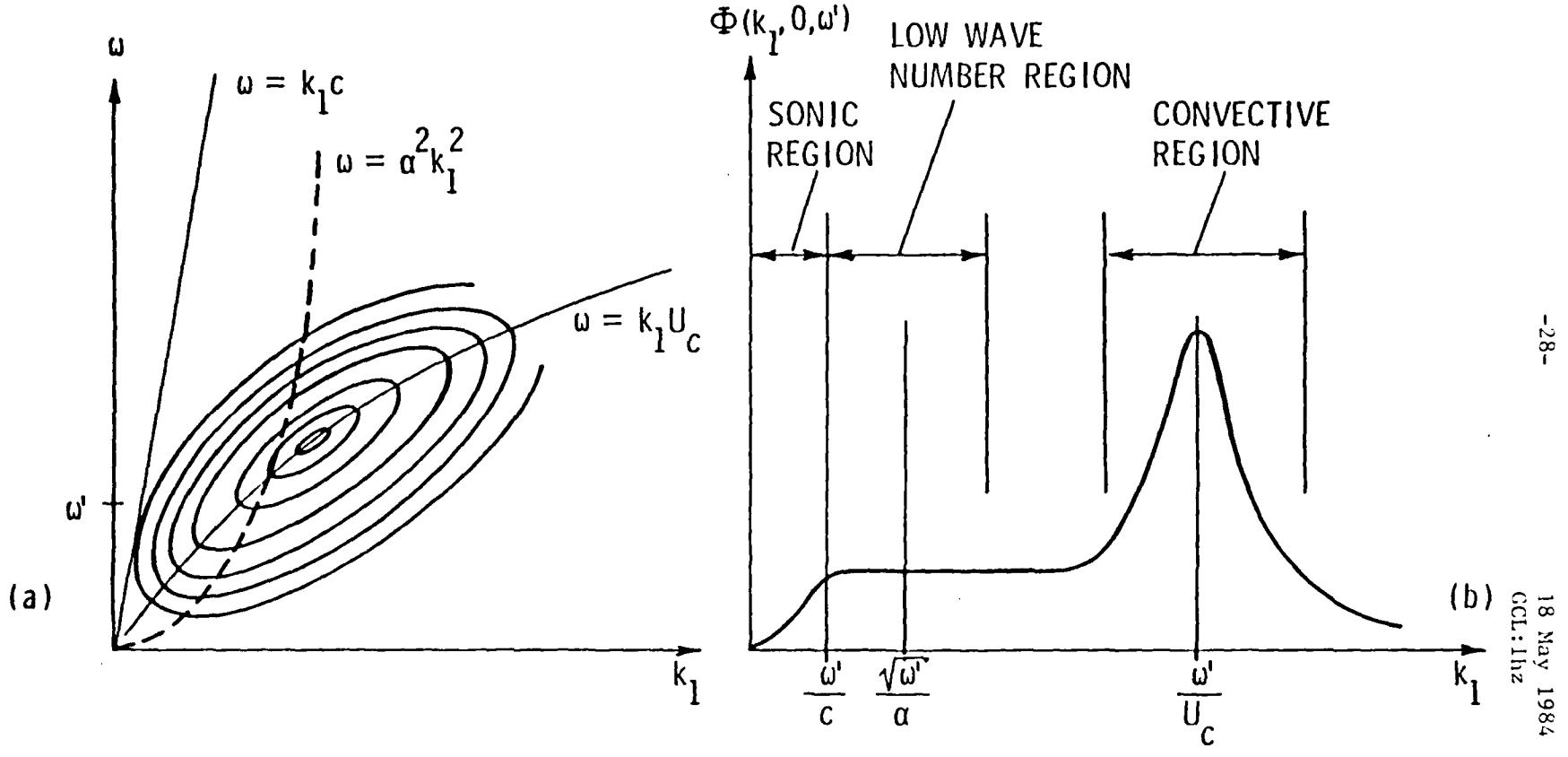

Figure 4. Schematic description of the wavenumber/frequency spectrum, where (a) shows the ω - k_1 plane and (b) shows the Φ - k_1 plane.

18 May 1984
GCL:lhz

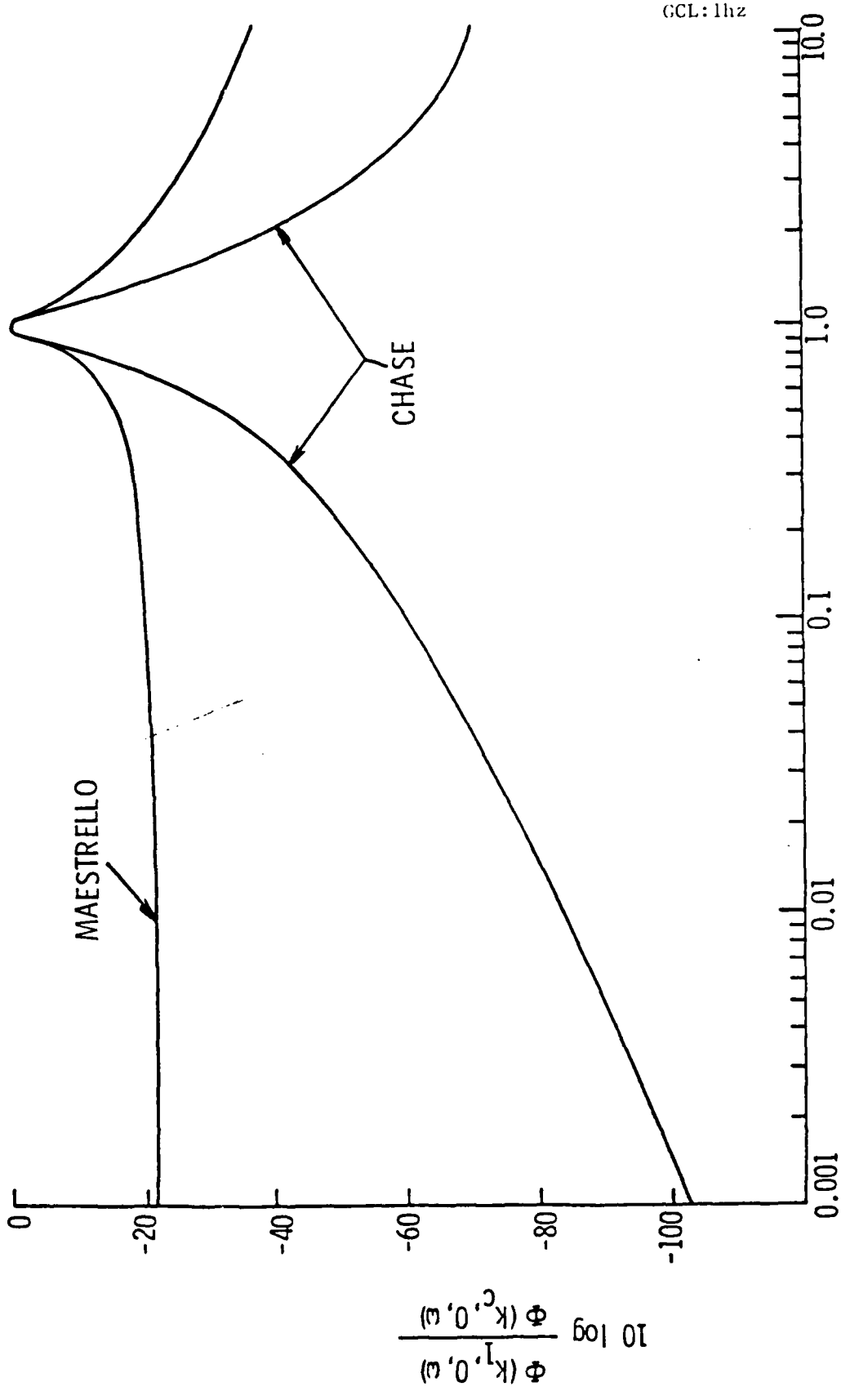

Figure 5. Theoretical wavenumber/frequency spectra based on the models of Maestrello [17] and Chase [18].

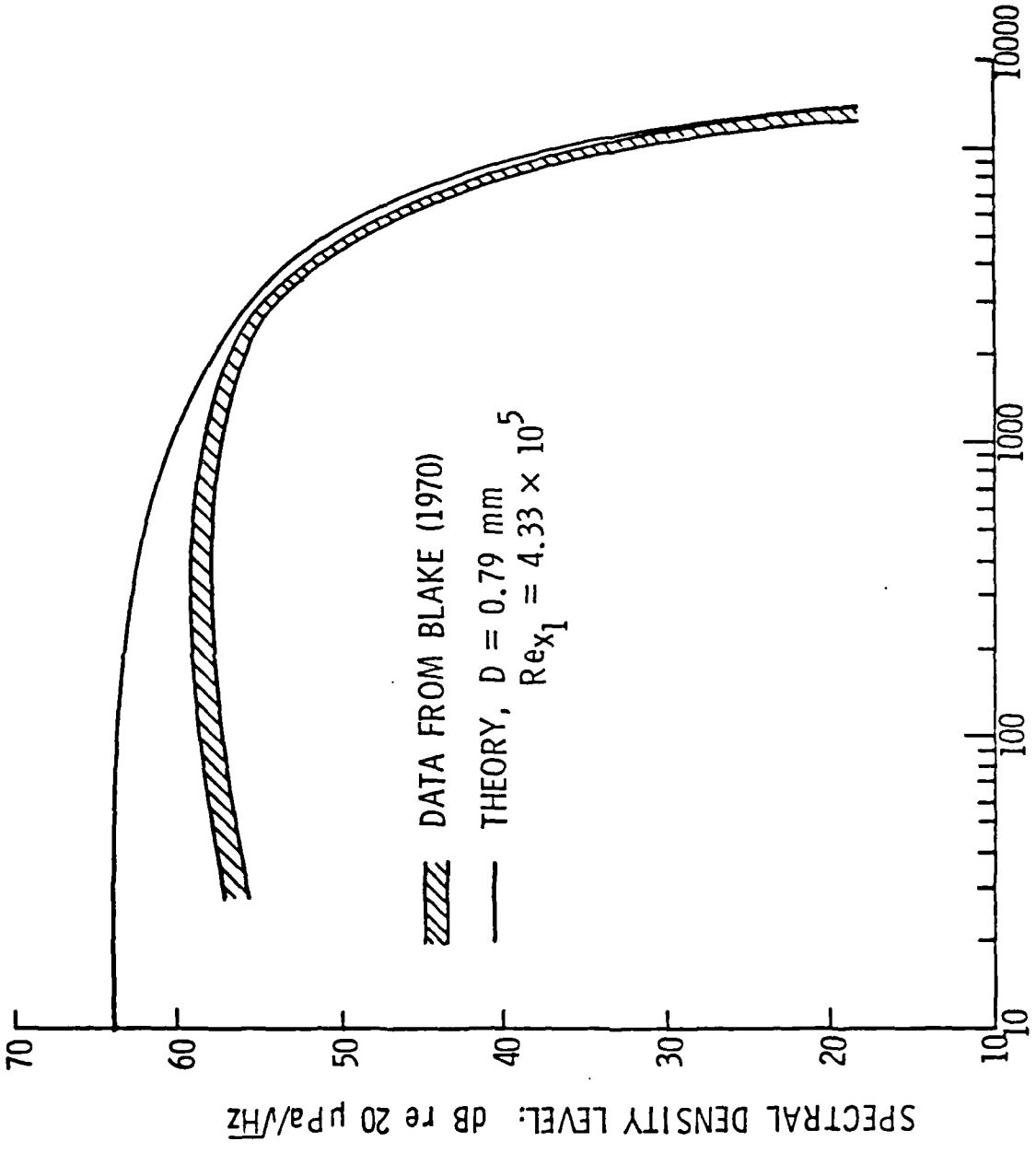

Figure 6. A comparison of the wall pressure spectrum measured by Blake [15] with a theoretical prediction based on Equation (A-1) and the Chase [18] model for $\Phi(k_1, k_3, \omega)$.

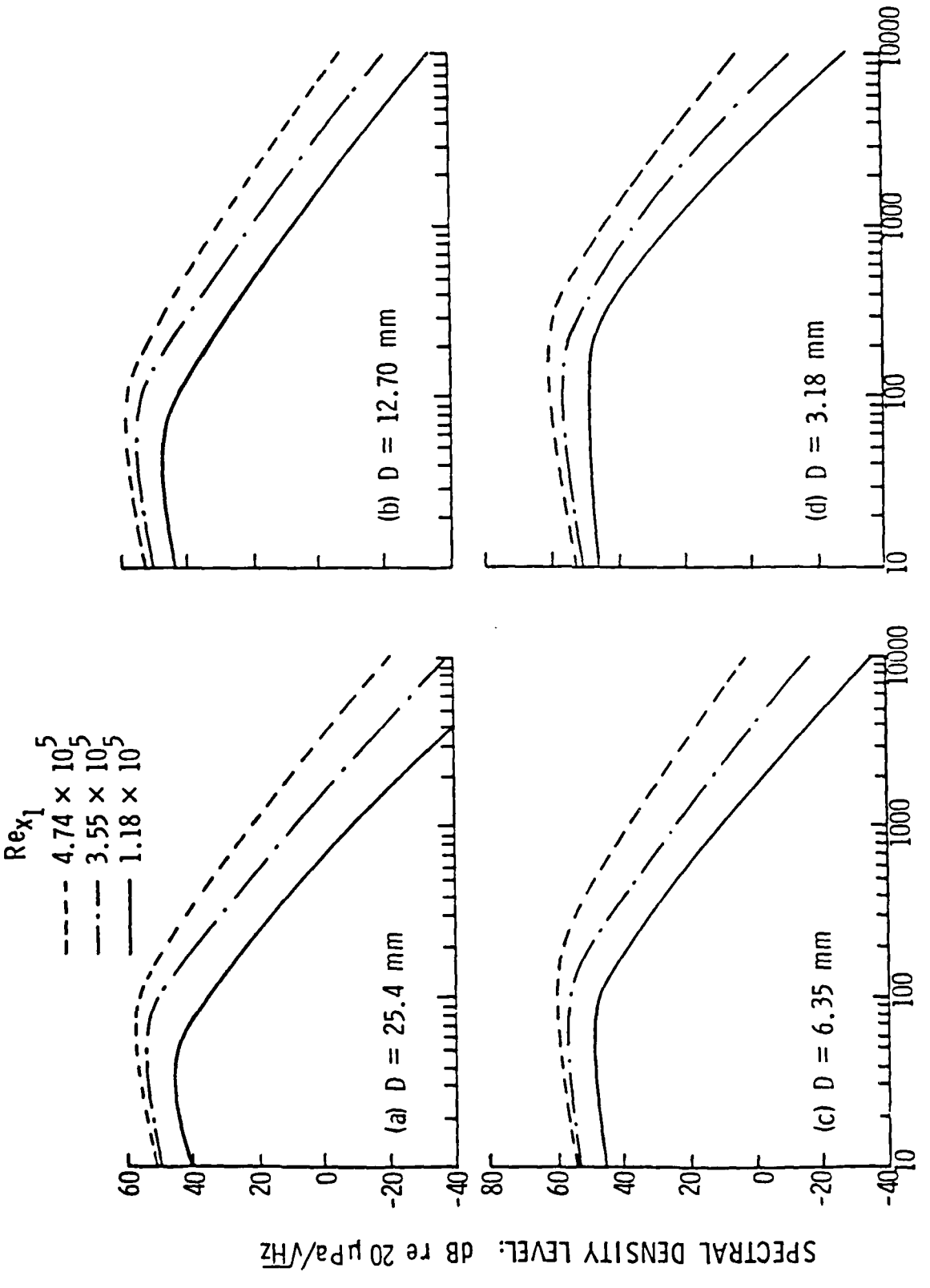

Figure 7. Example calculations of $G_{TT}(\omega)$ for various values of the flow Reynolds number and for sensor diameters: (a) 25.40 mm, (b) 12.70 mm, (c) 6.35 mm, and (d) 3.18 mm.

DISTRIBUTION LIST FOR UNCLASSIFIED TECHNICAL MEMORANDUM FILE NO. 84-87, by G. C. Lauchle, dated 18 May 1984

Commander
Naval Sea Systems Command
Department of the Navy
Washington, DC 20362
Attn: Library
Code NSEA-09G32
(Copies 1 and 2)

Commander
Naval Sea Systems Command
Department of the Navy
Washington, DC 20362
Attn: R. Keane
Code NSEA-3213
(Copy No. 3)

Commander
Naval Sea Systems Command
Department of the Navy
Washington, DC 20362
Attn: A. R. Paladino
Code NSEA-55N
(Copy No. 4)

Commander
Naval Sea Systems Command
Department of the Navy
Washington, DC 20362
Attn: F. B. Peterson
Code NSEA-052P
(Copy No. 5)

Commander
Naval Sea Systems Command
Department of the Navy
Washington, DC 20362
Attn: C. D. Smith
Code NSEA 63R
(Copy No. 6)

Commander
Naval Sea Systems Command
Department of the Navy
Washington, DC 20362
Attn: D. C. Houser
Code NSEA-63R14
(Copy No. 7)

Commander
Naval Sea Systems Command
Department of the Navy
Washington, DC 20362
Attn: F. J. Romano
Code NSEA-63R3
(Copy No. 8)

Commander
Naval Sea Systems Command
Department of the Navy
Washington, DC 20362
Attn: T. E. Peirce
Code NSEA 63R31
(Copy No. 9)

Commander
Naval Sea Systems Command
Department of the Navy
Washington, DC 20362
Attn: S. Silverstein
Code NSEA-63Y1
(Copy No. 10)

Commander
Naval Sea Systems Command
Department of the Navy
Washington, DC 20362
Attn: E. G. Liszka
Code PMS-406B
(Copy No. 11)

Commanding Officer
Naval Underwater Systems Center
Department of the Navy
Newport, RI 02840
Attn: B. J. Meyers
Code 36311
(Copy No. 12)

Commanding Officer
Naval Underwater Systems Center
Department of the Navy
Newport, RI 02840
Attn: T. A. Davis
Code 36314
(Copy No. 13)

DISTRIBUTION LIST FOR UNCLASSIFIED TECHNICAL MEMORANDUM FILE NO. 84-87, by G. C. Lauchle, dated 18 May 1984 [continuation]

Commanding Officer
Naval Underwater Systems Center
Department of the Navy
Newport, RI 02840
Attn: D. Goodrich
Code 3634
(Copy No. 14)

Commanding Officer
Naval Underwater Systems Center
Department of the Navy
Newport, RI 02840
Attn: C. Hervey
Code 3634
(Copy No. 15)

Commanding Officer
Naval Underwater Systems Center
Department of the Navy
Newport, RI 02840
Attn: R. H. Nadolink
Code 3634
(Copy No. 16)

Commanding Officer
Naval Underwater Systems Center
Department of the Navy
Newport, RI 02840
Attn: Library
Code 54
(Copy No. 17)

Commander
David W. Taylor Naval Ship
Research & Development Center
Department of the Navy
Bethesda, MD 20084
Attn: V. J. Monacella
Code 1504
(Copy No. 18)

Commander
David W. Taylor Naval Ship
Research & Development Center
Department of the Navy
Bethesda, MD 20084
Attn: Library
Code 1505
(Copy No. 19)

Commander
David W. Taylor Naval Ship
Research & Development Center
Department of the Navy
Bethesda, MD 20084
Attn: J. H. McCarthy
Code 154
(Copy No. 20)

Commander
David W. Taylor Naval Ship
Research & Development Center
Department of the Navy
Bethesda, MD 20084
Attn: M. M. Sevik
Code 19
(Copy No. 21)

Commander
David W. Taylor Naval Ship
Research & Development Center
Department of the Navy
Bethesda, MD 20084
Attn: M. Strasberg
Code 1901
(Copy No. 22)

Commander
David W. Taylor Naval Ship
Research & Development Center
Department of the Navy
Bethesda, MD 20084
Attn: W. K. Blake
Code 1950
(Copy No. 23)

Commander
David W. Taylor Naval Ship
Research & Development Center
Department of the Navy
Bethesda, MD 20084
Attn: D. Feit
Code 1960
(Copy No. 24)

DISTRIBUTION LIST FOR UNCLASSIFIED TECHNICAL MEMORANDUM FILE NO. 84-87, by G. C. Lauchle, dated 18 May 1984 [continuation]

Commander
David W. Taylor Naval Ship
Research & Development Center
Department of the Navy
Bethesda, MD 20084
Attn: R. A. Rippeon
Code 1980
(Copy No. 25)

Commander
David W. Taylor Naval Ship
Research & Development Center
Department of the Navy
Bethesda, MD 20084
Attn: F. S. Archibald
Code 1942
(Copy No. 26)

Commander
David W. Taylor Naval Ship
Research & Development Center
Department of the Navy
Bethesda, MD 20084
Attn: T. M. Farabee
Code 1942
(Copy No. 27)

Commander
David W. Taylor Naval Ship
Research & Development Center
Department of the Navy
Bethesda, MD 20084
Attn: F. E. Geib
Code 1942
(Copy No. 28)

Commanding Officer
Naval Undersea Warfare
Engineering Station
Department of the Navy
Keyport, WA 98345
Attn: Library
(Copy No. 29)

Commander
Naval Surface Weapons Center
Department of the Navy
Silver Spring, MD 20910
Attn: G. C. Gaunaurd
Code R-31
(Copy No. 30)

Commander
Naval Surface Weapons Center
Department of the Navy
Silver Spring, MD 20910
Attn: Library
(Copy No. 31)

Office of Naval Research
800 North Quincy Street
Department of the Navy
Arlington, VA 22217
Attn: M. M. Reischman
Code 432F
(Copy No. 32)

Commanding Officer
Naval Ocean Systems Center
Department of the Navy
San Diego, CA 92152
Attn: E. W. Hendricks
Code 6342
(Copy No. 33)

Commanding Officer
Naval Ocean Systems Center
Department of the Navy
San Diego, CA 92152
Attn: D. M. Ladd
Code 6342
(Copy No. 34)

Commanding Officer
Naval Ocean Systems Center
Department of the Navy
San Diego, CA 92152
Attn: Library
(Copy No. 35)

Commander
Naval Coastal Systems Center
Department of the Navy
Panama City, FL 32407
Attn: M. Hyman
Code 4210
(Copy No. 36)

DISTRIBUTION LIST FOR UNCLASSIFIED TECHNICAL MEMORANDUM FILE NO. 84-87, by G. C. Lauchle, dated 18 May 1984 [continuation]

Defense Technical Information Center
5010 Duke Street
Cameron Station
Alexandria, VA 22314
(Copies 37 through 42)

Westinghouse Electric Corp.
Post Office Box 1488
Annapolis, MD 21404
Attn: Dr. R. F. Mons
(Copy No. 43)

NASA Langley Research Center
Hampton, VA 22665
Attn: Dr. L. Maestrello
(Copy No. 44)

Dr. R. J. Hansen
Naval Research Laboratory
Marine Technical Division
Washington, DC 20390
(Copy No. 45)

Mr. P. S. Klebanoff
National Bureau of Standards
Aerodynamics Section
Washington, DC 20234
(Copy No. 46)

Professor D. G. Crighton
University of Leeds
Dept. Appl. Math. Studies
Leeds LS29JT
England
(Copy No. 47)

Dr. N. A. Brown
Bolt, Beranek and Newman
50 Moulton Street
Cambridge, MA 02136
(Copy No. 48)

Dr. K. L. Chandiramani
Bolt, Beranek and Newman
50 Moulton Street
Cambridge, MA 02136
(Copy No. 49)

Professor P. Leehey
Dept. of Ocean Engineering
Massachusetts Institute of Technology
77 Massachusetts Avenue
Cambridge, MA 02139
(Copy No. 50)

Professor J. L. Lumley
Sibley School of Mechanical & Aeronautical Engineering
Upson Hall
Cornell University
Ithaca, NY 14850
(Copy No. 51)

Dr. R. E. A. Arndt
St. Anthony Falls Hydraulic Lab
University of Minnesota
Mississippi River at 3rd Ave., S.E.
Minneaspolis, MN 55414
(Copy No. 52)

Professor V. J. Arakeri
Dept. of Mechanical Engineering
Indian Institute of Science
Bangalore 560 012
India
(Copy No. 53)

Dr. W. W. Haigh
Dynamics Technology, Inc.
22939 Hawthorne Blvd.
Suite 200
Torrance, CA 90503
(Copy No. 54)

Professor M. Pierucci
Dept. of Aerospace Engineering and Engineering Mechanics
San Diego State University
San Diego, CA 92182
(Copy No. 55)

Professor Eli Reshotko
Case Western Reserve University
Cleveland, OH 44106
(Copy No. 56)

DISTRIBUTION LIST FOR UNCLASSIFIED TECHNICAL MEMORANDUM FILE NO. 84-87, by G. C. Lauchle, dated 18 May 1984 [continuation]

Dr. W. W. Lang
IBM Corporation
Acoustics Laboratory
Post Office Box 390
Building 704
Poughkeepskie, NY 12602
(Copy No. 57)

Mr. D. Yeager
IBM Corporation
Acoustics Laboratory
Post Office Box 390
Building 704
Poughkeepskie, NY 12602
(Copy No. 58)

Mr. Francois Jouaillec
Office National d'Etudes et de
Recherches Aerospatiales
(ONERA)
Direction de la Physique Generale
BP 72
92322 Chatillon Cedex
(Copy No. 59)

Dr. Massot
Science Industries
22 Avenue Liberation
Montereau 77130
France
(Copy No. 60)

Mr. Glen Steyer
Structural Dynamics Research
Corporation
2000 Eastman Drive
Milford, OH 45150
(Copy No. 61)

Dr. George F. Kuhn
Vibrasound Research Corporation
10957 East Bethany Drive
Aurora, Colorado 80014
(Copy No. 62)

Dr. Eric Stusnick
Wyle Laboratories
The Hayes Building, Suite 404
2361 Jefferson Davis Highway
Arlington, VA 22202
(Copy No. 63)

Dr. Pritchard White
Bolt Beranek and Newman, Inc.
21120 Vanowen Street
Post Office Box 633
Canoga Park, CA 91305
(Copy No. 64)

Director
Applied Research Laboratory
The Pennsylvania State University
Post Office Box 30
State College, PA 16804
Attn: L. R. Hettche
(Copy No. 65)

Director
Applied Research Laboratory
The Pennsylvania State University
Post Office Box 30
State College, PA 16804
Attn: G. C. Lauchle
(Copy No. 66)

Director
Applied Research Laboratory
The Pennsylvania State University
Post Office Box 30
State College, PA 16804
Attn: B. R. Parkin
(Copy No. 67)

Director
Applied Research Laboratory
The Pennsylvania State University
Post Office Box 30
State College, PA 16804
Attn: E. J. Skudrzyk
(Copy No. 68)

DISTRIBUTION LIST FOR UNCLASSIFIED TECHNICAL MEMORANDUM FILE NO. 84-87, by G. C. Lauchle, dated 18 May 1984 [continuation]

Director
Applied Research Laboratory
The Pennsylvania State University
Post Office Box 30
State College, PA 16804
Attn: ARL/PSU Library
(Copy No. 69)

Director
Applied Research Laboratory
The Pennsylvania State University
Post Office Box 30
State College, PA 16804
Attn: GTWT Files
(Copy No. 70)

Mr. Kirby Miller
Advanced Technologies
Western Division
GTE Government Systems
Corporation
100 Ferguson Drive
Post Office Box 7188
Mountain View, CA 94039
(Copy No. 71)

Mr. Alan G. Piersol
Bolt Beranek and Newman, Inc.
21120 Vanowen Street
Canoga Park, CA 91303
(Copy No. 72)

Professor Dr. H. Myncke
Laboratorium Voor Akoestiek
En Warmtegeleiding
Celestijnenlaan 200 D
B-3030 Heverlee
Belgium
(Copy No. 73)